ACS OMEGA

Open Access

This article is licensed under CC-BY-NC-ND 4.0

http://pubs.acs.org/journal/acsodf

Article

Physicochemical Properties of Carbon Fiber Formulated from Melt-Spun Raw Asphaltene

Shahrad Khodaei Booran, Jiawei Chen, Md Minhajul Islam, Idaresit Ekaette, TriDung Ngo, Mark McDermott, Tian Tang, and Cagri Ayranci*

Cite This: *ACS Omega* 2024, 9, 50318−50325

Read Online

ACCESS | Metrics & More | Article Recommendations | Supporting Information

ABSTRACT: One of the challenges in carbon fiber production centers around the high cost of raw materials required for fiber precursors or complex production processes involving multiple steps. This research paper delves into the utilization of asphaltene sourced from Alberta oil sands as an alternative precursor material that is low cost for carbon fiber production. We investigated the carbon fiber production process using a blend of different asphaltene types via melt-spinning technology. Carbon fibers produced from asphaltene-based precursors exhibit an average diameter of 12.66 ± 3.06 μm, an ultimate tensile strength (UTS) of 524.07 ± 218.53 MPa, an elastic modulus of 34.68 ± 15.61 GPa, and a strain at the UTS of 2.48 ± 0.97%. The results validate the viability of asphaltene as a precursor fiber and highlight the potential of carbon fibers.

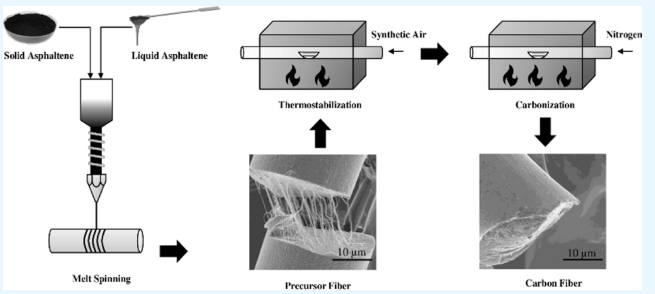

Downloaded via 121.86.30.74 on December 27, 2024 at 07:10:48 (UTC).
See https://pubs.acs.org/sharingguidelines for options on how to legitimately share published articles.

1. INTRODUCTION

Carbon fiber is primarily used as a reinforcing element in advanced composite materials across industries, such as aerospace, transportation, and sports. It offers high strength and stiffness, low coefficient of thermal expansion, exceptional heat resistance, and excellent chemical resistance. Due to these superior properties, global demand for carbon fiber is expected to exceed 285,000 tons per year by 2025.[1]

With high market demand, carbon fiber production has been extensively investigated in industry and academia. Manufacturing carbon fibers consists of several essential steps: producing precursor fibers, thermal stabilization, and carbonization. The precursor materials are primarily derived from rayon, pitch, and Polyacrylonitrile (PAN).[2,3] However, major drawbacks of commercial carbon fibers include the high cost of materials and complex multistep production processes. For example, for PAN-based carbon fiber, the materials make up more than 50% of the total cost of carbon fiber production.[4] Thus, finding more abundant materials as a precursor for carbon fiber production has gained considerable attention in recent years. Among the alternative materials, there are inexpensive resources such as biomass (cellulose and lignin), coal and petroleum by-products,[5,6] which can produce reasonably strong carbon fibers. Asphaltene is one such low-cost alternative,[7−11] as a side product of petroleum production.

Asphaltene is a solubility class of petroleum, defined as a precipitation fraction from specific solvents.[10] It is soluble in light aromatics such as benzene or toluene and insoluble in light paraffins such as pentane, hexane, and heptane.[8,9] As an unwanted part of petroleum industry, asphaltene aggregates and precipitates, which can lead to technical and economic problems, including clogging or damaging pipelines and distillation columns and poisoning catalysts during production operation.[12−14] In general, asphaltenes may contain 10^5 to 10^6 individual chemical species in different concentration, such as iso- and *n*-alkanes, cycloalkanes, and alkyl-cycloalkanes with rings of 3 to 8 carbons, alkyl benzenes, alkyl phenanthrenes, and a lower concentration of heteroatomic hydrocarbons that contain nitrogen, oxygen, and sulfur.[15−17] In contrast to other constituents within crude oil, asphaltene stands out as the densest and most polar fraction. Based on material characterizations including carbon content, aromaticity, heteroatom content, polar functional groups, and double bond equivalent numbers, asphaltene has been identified as a strong candidate for carbon fiber production.[7,18]

Melt spinning is one of the common and simple techniques to fabricate precursor fibers without using solvents; however, this technique requires good control of processing parameters such as melt viscosity, temperature, and collection speed.

Saad et al. fabricated carbon fibers from two types of asphaltenes, solid powder and solvent-extracted gel samples,

Received: July 12, 2024
Revised: October 29, 2024
Accepted: November 25, 2024
Published: December 11, 2024

© 2024 The Authors. Published by American Chemical Society

using *n*-pentane (sample/solvent ratio of 1:40). Only the properties of carbon fibers from solid asphaltene were reported: a fiber diameter of 30−100 μm, an elastic modulus of ∼70 GPa, and a tensile strength of ∼400 MPa.[9] Zuo et al. yielded better mechanical properties of asphaltene-based carbon fibers (elastic modulus of 71 GPa and tensile strength of ∼1130 MPa) from C5 asphaltene pretreated at 300 °C before melt spinning.[7] Leistenschneider et al. also reported that asphaltene-based carbon fibers could exhibit an elastic modulus of 32.7 GPa and a tensile strength of 811 MPa for C5 asphaltene pretreated with 40 vol % nitric acids.[8] These works demonstrate the feasibility of producing carbon fibers with good mechanical performance from asphaltenes and reducing the cost of carbon fibers. However, most of these works require acid or thermal pretreatments before thermal stabilization and carbonization. The addition of pretreatments not only increases the number of production steps but also can substantially raise the production cost of asphaltene-based carbon fiber, especially for mass production runs. To address the concerns of high manufacturing cost and negative environmental impact, reducing solvent usage in the asphaltene pretreatment process is paramount to the development of more sustainable processes.[19]

This paper explores the production of carbon fiber exclusively from Alberta's asphaltene, without the need for acid or thermal pretreatments, to streamline the production process. Asphaltene, characterized by its nonuniform composition and high melting point, typically requires a plasticizer to reduce melting temperature and viscosity, facilitating processing and minimizing degradation. To address these issues, we employed liquid asphaltene (LA) as a plasticizer to aid in the melt spinning of solid asphaltene (SA). These asphaltene samples are readily available as byproducts from the bitumen extraction process. Additionally, SA has previously been identified in our research as a precursor for carbon fiber production using a solution-processing method.[20]

2. EXPERIMENTAL DETAIL AND ANALYSIS

2.1. Materials. SA powder and LA were obtained from Alberta Innovates. Toluene (99.7%) was purchased from Fisher Scientific.

2.2. Precursor Fiber Preparation. The raw SA powder (100 g) was mixed with 2 L of toluene in a flask and then mixed for 3 h by a magnetic stirrer at 60 °C to obtain a uniform mixture. The mixture (SA/toluene) was initially filtered using a stainless-steel sieve (Fisherbrand U.S. Standard Stainless Steel Test Sieves, 12 in. diameter × 3.25 in. *D*, pore size 25 μm), followed by filter paper (Whatman 1001−110 Qualitative Filter Papers, pore size 11 μm). This process removed most impurities from asphaltene and prevented damage to the equipment (clogging) during melt spinning. The LA sample was cleaned by following the same process.

After cleaning, SA and LA were mixed in a flask (4 L) at different ratios for 3 h. Next, a rotovap (IKA rotary evaporator, RV 3) at a water bath temperature of 60 °C and rotating speed of 80 rpm was used to remove most of the toluene. The mixture was then air-dried for at least 96 h (4 days) to ensure evaporation of the residual toluene.

A twin-screw extruder with a 500 μm nozzle (Figure 1) was used to produce the asphaltene-based precursor fiber. The nozzle size smaller than 500 μm induced clogging. The extruder has three heating zones, where T1, T2, and T3 (closest to the nozzle) are the temperatures in each zone. For each preparation condition, the SA/LA ratio was tested from 0% to 40% to produce a reliable precursor fiber. The precursor fibers were produced from this extruder at least three times to ensure production repeatability.

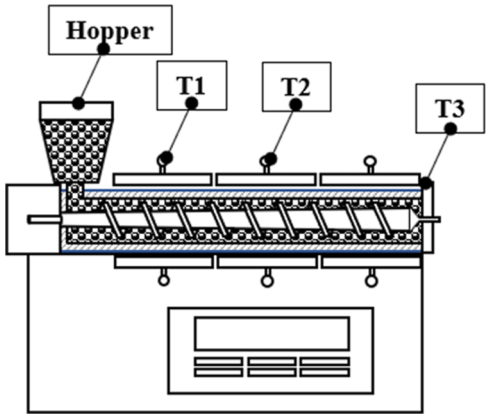

Figure 1. Experimental setup of a twin-screw extruder melt spinner.

2.3. Thermal Stabilization and Carbonization. A three-step thermal stabilization was applied where the produced precursor fibers were placed inside a ceramic boat and heated by a tube furnace (Thermo Scientific, Lindberg/Blue M Mini-Mite Tube Furnaces) from 25 to 100 °C (0.1 °C/min, 5 h), from 100 to 200 °C (0.25 °C/min, 1 h), and then from 200 to 300 °C (0.5 °C/min, 1 h). The thermostabilized fibers were finally cooled down from 300 to 25 °C at 5 °C/min under a controlled ultra-zero synthetic air flow rate of 0.5 slpm (standard liter per minute) to prevent melting during carbonization. Carbonization of the thermostabilized fibers was carried out by injecting nitrogen gas inside the furnace and heating it up from 25 to 300 °C (0.5 °C/min, 1 h) followed by 300 to 1000 °C (2 °C/min, 1 h). Lastly, the carbonized fibers were cooled down from 1000 to 25 °C at 5 °C/min.

2.4. Mass Spectroscopy. The cleaned SA and LA were dissolved in dichloromethane, followed by spotting 1 μL of the solution on a Bruker nanostructured laser desorption ionization platform (Bruker Daltonics, Billerica, MA, USA). Then, the samples were analyzed in an ultrafleXtreme MALDI−TOF/TOF mass spectrometer (Bruker Daltonics, Billerica, MA, USA).

2.5. Differential Scanning Calorimetry and Thermogravimetric Analysis. A differential scanning calorimetry (DSC) instrument (PerkinElmer Pyris DSC, Norwalk, CT, USA) was employed to characterize the thermal properties of the precursor fiber. The precursor fiber (about 2.5 mg), kept in a sealed aluminum pan, was heated from 25 to 600 °C at a heating rate of 10 °C/min under a nitrogen environment.

To further analyze the thermal behaviors of the precursor and thermostabilized fibers, thermogravimetric analysis (TGA) was carried out using a Mettler Toledo TGA/DSC 1 Star System (Switzerland) under nitrogen from 25 to 900 °C at a heating rate of 10 °C/min.

2.6. Microscopy. The fiber diameter was measured by an optical microscope (Olympus IX83). For the morphological study, the fibers produced at the three stages (precursor, thermally stabilized, and carbonized) were coated with gold by Denton Gold Sputter and observed with a Hitachi S-4800 Field Emission Scanning Electron Microscope at an accelerating voltage of 5 kV.

Furthermore, energy-dispersive X-ray analysis (EDS) with a Zeiss EVO MA10 SEM microscope was employed to study the

https://doi.org/10.1021/acsomega.4c06464
ACS Omega 2024, 9, 50318−50325

surface composition of the fibers. EDS was conducted at a voltage of 20 kV to identify the elements on the fiber cross-section with an 8.5 mm working distance. Lastly, energy-dispersive X-ray spectroscopy (EXD) was also implemented to map a cross-section of the precursor fiber in the epoxy matrix.

2.7. Elemental (CHNS/O) Analysis. To analyze the compositions of asphaltene-based fibers (precursor, thermally stabilized, and carbonized), a Flash 2000 CHNS/O Organic Elemental Analyzer (Thermo Fisher; Cambridge, UK) was used to measure the carbon, hydrogen, nitrogen, sulfur, and oxygen contents of the samples.

2.8. Fourier-Transform Infrared Spectroscopy. The Fourier-transform infrared spectroscopy (FTIR) spectra of cleaned SA powder, precursor, and carbonized fiber were recorded using a Nicolet 8700 Spectrophotometer (Thermo Fisher, USA) within the 400−4000 cm^{-1} spectral region, with 32 scans recorded at a 4 cm^{-1} resolution in the transmittance mode.

2.9. Raman Spectroscopy. Raman spectra of precursor fibers and carbonized fibers were analyzed using a Renishaw InVia Raman microscope with a 50× objective lens, 532 nm laser wavelength at 5% power, 1200 L/mm grating, exposure time of 4 s, accumulations of 50, and wavenumber from 800 to 2400 cm^{-1}. The data were collected with Wire 5.5 software.

2.10. X-ray Diffraction Analysis. The Rigaku Ultima IV X-ray diffraction (XRD) system equipped with a copper (Cu) source operating at 40 kV and 40 mA was employed to examine the carbon structure of the fibers. The spectra were obtained in the range 5−90° at a rate of 2°/min with a 0.05° sampling step and 5 mm DHL slit.

2.11. Mechanical Test. Mechanical characterization of individual carbon fibers was conducted with an ElectroForce tensile machine (BOSE Corporation, USA). The procedure to prepare samples for the tensile test is shown in Figure 2. A

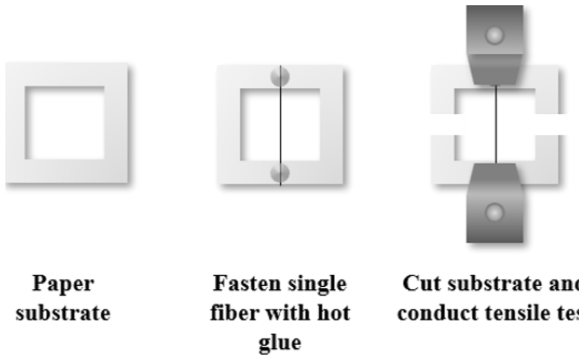

Figure 2. Tensile test specimen preparation.

carbon fiber specimen was fastened by using hot glue to the middle of a rectangular paper frame with a gap of 5 mm and a frame thickness of 10 mm. Then, the paper frame was mounted on the tensile grippers, the vertical sides were cut, and the uniaxial load was measured with a 250 *g*-limit load cell. The strain was reported as the ratio of the sample elongation divided by the initial gage length (5 mm). The stress was calculated as the force divided by the cross-section area of the fiber measured by an Olympus IX 83 microscope.

3. RESULTS AND DISCUSSION

3.1. Melt Spinning of Precursor Fibers. Melt-spinning-cleaned SA presents a considerable challenge due to its high melting point. This elevated melting point demands substantial energy input during the extrusion process. To address this challenge, LA was introduced as a plasticizer to reduce the melting point of the precursor mixture, making it more suitable for the melt-spinning process.

The mass spectral analysis of the SA and LA samples, as depicted in Figure 3a, offers valuable insights. The spectra reveal a diverse distribution of molecular weights (MWs) in both sample sets. Notably, LA demonstrates a notably lower average MW compared to its SA counterpart. This variance in MW leads to a considerable reduction in viscosity and a corresponding decrease in the melting point for LA, rendering it a more adaptable candidate for the melt-spinning process. Based on a series of preliminary tests, SA/LA of 35% was identified as an optimal ratio that renders a moderate melting temperature (235 °C).

Figure 3b illustrates the phase-transition temperatures of precursor fibers obtained from the melt-spun asphaltene. The recorded endothermic peaks within the range of 130 to 180 °C can be attributed to the glass transition or softening of the amorphous components, which are characterized by their lower polarity, in the asphaltene.[21] Another endothermic phase transition occurs around 260 °C, signifying the melting of the crystalline fractions of asphaltene, which possess a higher polarity. Additionally, at temperatures ranging from 470 to 480 °C, asphaltene undergoes a decomposition or pyrolysis process.[22] Based on these data, the operational temperatures were chosen to be less than 260 °C. More specifically, T1, T2, and T3 were set to 50, 165, and 223 °C, respectively, as these were found to produce thin and uniform precursor fibers, without nozzle clogging or fiber breakage.

Fiber spooler speed (in millimeters per second) is also a crucial parameter for determining the diameter of the melt-spun fibers. As shown in Figure 3c, when the spooler speed increased from 1250 to 3300 mm/s, the average precursor fiber diameter drastically decreased from 54.4 ± 7.14 μm to 19.6 ± 7.32 μm. Above 3300 mm/s, the fiber diameter shows a more gradual decrease with increasing spooler speed. Beyond the spooler speed of 5500 mm/s, continuous fiber production was not feasible.

Another important parameter that influences the precursor fiber diameter is the extruder's screw speed. Lower extruder speed ensures a longer residence time and more prolonged heat exposure for the asphaltene powders in the heating chamber. By decreasing the extruder speed from 15 to 10 rpm, the average precursor fiber diameter decreased by 23.4% (from 71.01 μm ± 8.44 to 54.4 μm ± 7.14 μm), but a further reduction in the extruder speed interrupted fiber production.

Based on the above studies, the best operational conditions for the SA/LA (35%) mixture were determined to be T1 = 50 °C/T2 = 165 °C/T3 = 223 °C, extruder speed of 10 rpm, and spooler speed of 5300 mm/s on the extruder.

3.2. Thermostabilization and Carbonization. Different temperature levels, heating rates, and residence times were optimized for the thermal stabilization and carbonization processes. Prior to heat treatment, the cross-section of the precursor fiber reveals subfilaments that remain unbroken, connecting the fiber segments under tension, as depicted in Figure 4a. The subfilaments are attributed to the presence of LA, which allows the spinner to stretch the precursor fiber at high speed continuously without breakage. The precursor fiber shows slight indentations on the surface (Figure 4d) as evaporation of residual toluene in the asphaltene feed generates small pores. During the extrusion, the stretching force elongates the pores

https://doi.org/10.1021/acsomega.4c06464
ACS Omega 2024, 9, 50318−50325

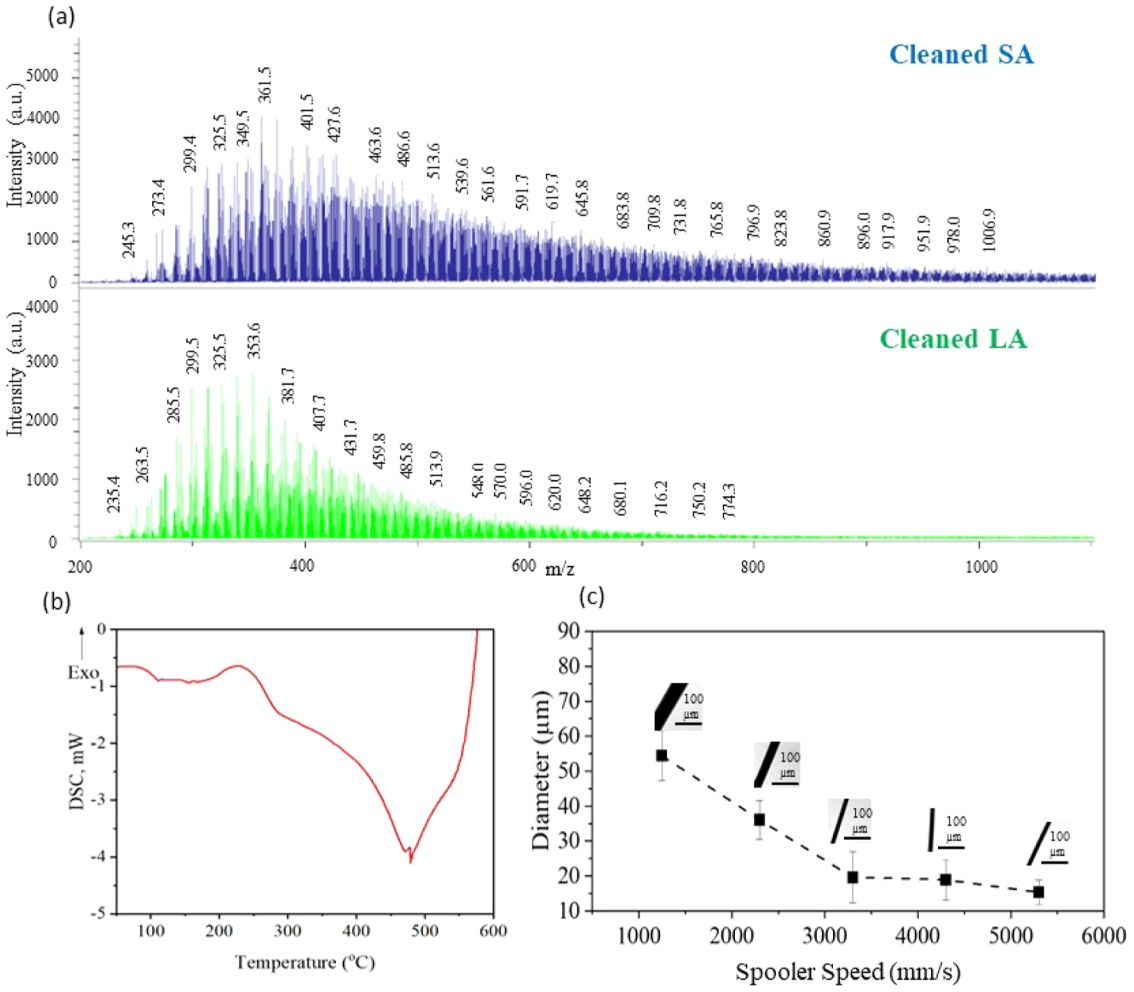

Figure 3. (a) Mass spectra of cleaned SA and LA, (b) DSC curve of precursor fibers, and (c) diameter changes of the precursor fiber with spooler speed.

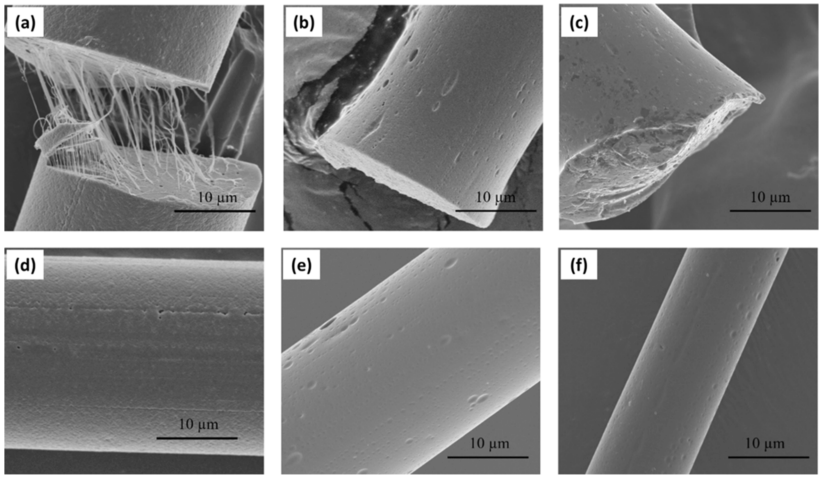

Figure 4. Cross-sectional morphology and diameter of the precursor fiber (a,d), thermostabilized fiber (b,e) (after three-step thermostabilization), and carbonized fiber (c,f) (25 to 300 °C (0.5 °C/min, 1 h) followed by 300 to 1000 °C (2 °C/min, 1 h)).

and leaves longitudinal indentations on the surface. Besides the three-step thermostabilization process described in Section 2.3, a two-step thermostabilization was also attempted, where the precursor fiber was heated from 25 to 100 °C (0.1 °C/min, 5 h) and then from 100 to 300 °C (0.5 °C/min, 1 h). The thermostabilized fibers were then cooled down from 300 to 25 °C at 5 °C/min. The fibers treated with the two-stage thermostabilization exhibited significant cracks on the surface (Supporting Information Figure S1). However, by incorporating an additional stage at 200 °C with a lower heating rate, the fibers displayed a markedly smoother surface with significantly fewer defects, though minor imperfections and surface voids were still visible (Figure 4b,e). This adjustment represents a substantial

https://doi.org/10.1021/acsomega.4c06464
ACS Omega 2024, 9, 50318−50325

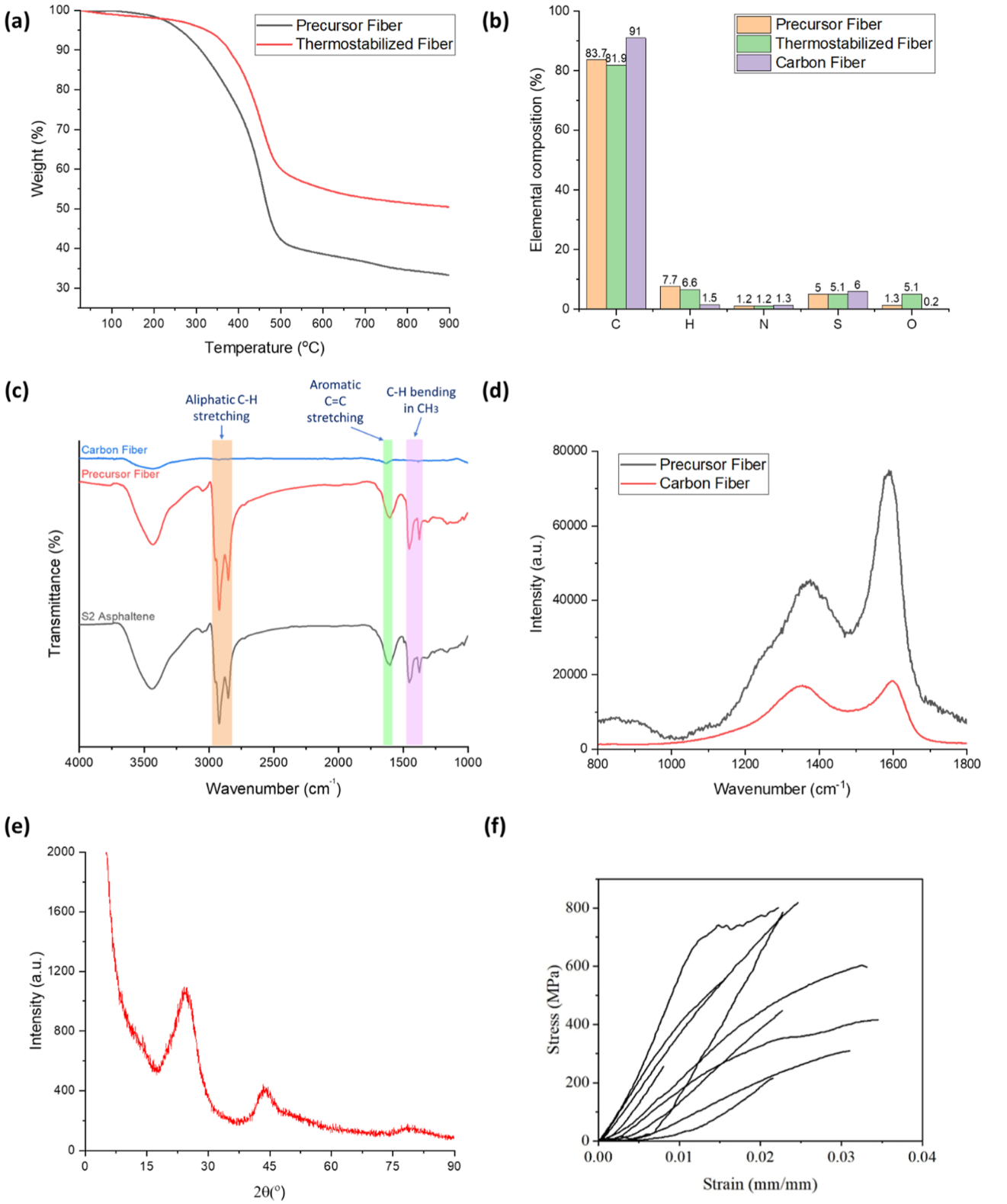

Figure 5. Analytical characterizations: (a) TGA thermograms of precursor and thermal-stabilized fibers, (b) CHNS/O elemental analysis for precursor, thermo-stabilized, and carbon fibers, (c) FTIR spectra of cleaned SA, precursor, and carbonized fibers, (d) Raman spectra of precursor and carbonized fibers, (e) XRD pattern of carbonized fibers, and (f) tensile test results showing stress−strain curves of all ten samples cut off at their respective ultimate tensile strength (UTS).

improvement in fiber quality compared with the two-step process.

According to Figure 4b, the LA subfilaments at cross-section of thermostabilized fibers disappeared, which may be due to complete oxidation of fibers during thermal stabilization. Lastly, the carbonized fiber (Figure 4c,f) shows a smooth surface and mostly a pore-free cross-section. The average diameter decreases

https://doi.org/10.1021/acsomega.4c06464
ACS Omega 2024, 9, 50318−50325

by 75.62% from the precursor (51.92 ± 6.02 μm) to carbonized (12.66 ± 3.06 μm) fibers.

TGA results in Figure 5a provide insight into the thermal stability of both precursor and thermostabilized fibers. The precursor fiber maintains stability at lower temperatures, with only a minimal 1% weight loss observed up to 200 °C. Subsequently, between 200 and 400 °C, there is a 20% weight loss attributed to the evaporation of volatile components or the release of adsorbed gases from the asphaltenes. A significant 35% weight loss occurs between 400 and 500 °C, primarily due to asphaltene molecule decomposition and the liberation of volatiles from the asphaltene molecules, with a peak at 450 °C. In contrast, the thermostabilized fiber exhibits exceptional thermal stability, with only a minor 3% weight loss observed up to 300 °C, marking the upper limit of stabilization. Carbonization under nitrogen (inert environment) confirms a consistently maintained weight of about 50%. These results underscore the superior thermal stability and resistance to decomposition in thermostabilized fibers compared with their precursor counterparts.

The CHNS/O test was carried out to examine the elemental compositions of the precursor and thermostabilized and carbonized fibers. The precursor fiber displayed a carbon content of 83.7%, indicating that carbon-rich asphaltene is suitable for producing a carbon fiber. The carbon content in the carbonized fiber was even higher, measuring 7.3% and 9.1% more than the precursor and thermostabilized fibers, respectively (Figure 5b). The carbon fiber yielded an impressive carbon content of 91.0%, demonstrating the potential for commercializing carbon fiber derived from asphaltene. While the sulfur and nitrogen contents in the different fibers remained relatively consistent at 5−6% and 1.2−1.3%, respectively, the carbon fiber exhibited significantly lower levels of oxygen and hydrogen compared to the precursor fiber. This suggests that hydrogen and oxygen were released from the material as small volatile molecules, such as H_2O. The elemental composition of SA and LA is presented in the Supporting Information section (Supporting Information Figure S2). The results corresponding to the EDX analysis of precursor fibers are presented in the Supporting Information section (Supporting Information Figure S3), which show good agreement with the elemental analysis, indicating that the main composition of the precursor fibers includes C, N, S, and O.

Table 1 provides a summary of the elemental ratios of the fibers at different stages of thermal treatments expressed as percentages. Initially, the precursor fiber had an H/C ratio of approximately 9.9%. However, after carbonization, this ratio decreased to 1.7%. Additionally, the N/C and O/C ratios were relatively low in the carbonized fiber. These findings indicate a decrease in the quantity of aliphatic C−C single bonds and an increase in the formation of aromatic C═C double bonds. These changes can lead to the improved mechanical strength of the carbonized fiber when compared to the precursor fiber.

Table 1. Elemental Ratio (in Percentage) in Asphaltene-Based Fibers

	precursor fiber	thermo-stabilized fiber	carbon fiber
H/C	9.9	9.0	1.7
N/C	1.5	1.7	1.4
S/C	6.4	6.9	6.8
O/C	1.7	7.0	0.2

In Figure 5c, a comparison of FTIR spectra is presented among the cleaned SA, precursor fiber, and carbonized fiber. All samples, including asphaltene and its derived fibers, displayed distinct N−H or O−H stretching peaks within the wavenumber range of 3428 to 3441 cm^{-1}. However, a noticeable decrease in the peak area around ∼2852 cm^{-1} and ∼2923 cm^{-1}, corresponding to aliphatic C−H bond stretching vibrations, was observed throughout the thermal processes, eventually becoming negligible in the carbonized fiber. This reduction indicates a significant depletion of aliphatic chains in the carbonized fiber compared to the precursor and asphaltene.[7] Furthermore, the carbon fiber exhibited the highest aromaticity index, determined by the ratio between the area under the C−H aliphatic stretching peak in the 2770−3000 cm^{-1} region and the area under the C═C aromatic stretching band in the 1500−1630 cm^{-1} region.[23] This increased aromaticity index suggests a higher abundance of aromatic sheets or cyclic ring structures in the carbon fiber. Additionally, further analysis revealed that the intensities of the peaks at ∼1451 and 1388 cm^{-1}, representing C−H bending vibrations in the CH_2 scissoring mode, decreased from the precursor to the carbonized fiber. This trend indicates a decrease in the number of aliphatic chains and further supports the presence of more aromatic structures in the carbonized fiber.[7,23] This implies a reinforcement of aromatic C═C bonding, resulting in the carbon fiber being less brittle compared with the precursor asphaltene.

The Raman spectra of both precursor and carbonized fibers exhibit two distinctive bands associated with graphite crystallites, as depicted in Figure 5d. These bands are observed at the wave numbers of 1360−1370 cm^{-1} and ∼1590−1600 cm^{-1}, referred to as the D-band and G-band, respectively.[24] The G-band, which corresponds to the vibration of the graphitic ring structure, maintains a similar intensity in the carbonized fibers compared to the precursor fibers, indicating its presence and persistence throughout the thermal treatment process.[25] However, the intensity of the D-band, representing defects within the graphite crystalline structure, is higher in the carbon fiber than in the precursor fiber. This suggests a decrease in the degree of structural order resulting from the breakdown of symmetry and the presence of edge planes following carbonization.[25−27] The G/D ratios for the carbonized and precursor fibers are 1.07 and 1.26, respectively. This decrease in the G/D ratio after carbonization further confirms the increase in structural defects and the reduction in graphitic order, aligning with the observed increase in the D-band intensity.

The carbonized fiber was subjected to XRD analysis, revealing a clear and prominent peak at an angle of approximately 25° (Figure 5e). This peak signifies the presence of a specific crystallographic plane, known as (002),[28,29] which is characteristic of carbon materials. Throughout the carbonization process, the flat graphene-like structures arrange themselves in a stacked manner, facilitated by $\pi-\pi$ interactions, ultimately forming turbostratic graphitic crystallite structures within the carbon fiber.[27,28,30] Moreover, another peak was observed in the diffraction pattern of the carbonized fiber at approximately 44°, corresponding to the (100) plane found in the crystal structure of graphite. This peak arises from the organized arrangement of atoms within the graphitic planes.[31]

The stress−strain curves of all test samples up to the UTS are displayed in Figure 5f. The mechanical properties of the carbonized fibers were obtained from the stress−strain curves. The following properties were calculated: UTS of 524.07 ± 218.53 MPa, elastic modulus of 34.68 ± 15.61 GPa, and strain at

https://doi.org/10.1021/acsomega.4c06464
ACS Omega 2024, 9, 50318−50325

Table 2. Mechanical Properties of Melt-Spun Carbon Fibers Produced from Byproduct Precursors

precursor	byproduct industry	mechanical properties	references
eucalyptus tar pitch	charcoal manufacturing	UTS of 130 MPa elastic modulus of 14 GPa	34
hardwood kraft lignin	ethanol and pulp production	UTS of 510 MPa elastic modulus of 28.6 GPa	35
slurry oil (pitch)	catalytic cracking	UTS of 662.3 MPa elastic modulus of 47.65 GPa strain at break of 2.06%	36
softwood lignin O-acyl derivatives	ethanol and pulp production	UTS of 520 MPa elastic modulus of 41.1 GPa strain at break of 1.34%	37
asphaltene	crude oil production	UTS of 524.07 ± 218.53 MPa elastic modulus of 34.68 ± 15.61 GPa strain at UTS of 2.48 ± 0.97%	this work

UTS of 2.48 ± 0.97%. Compared to carbon fibers melt spun from other alternative precursors (byproduct precursors) (Table 2), asphaltene-based carbon fibers presented in this work showed comparable mechanical properties.[32,33] The melt-spun asphaltene carbon fibers produced in this work also demonstrate a potential for producing a value-added product from Alberta Oil Sand's Asphaltene as alternative carbon fibers.

4. CONCLUSIONS

The production of carbon fiber from asphaltene was accomplished through melt spinning without the need for additional aiding polymers or extensive chemical treatment. An extruder speed of 10 rpm and a spooler speed of 5300 mm/s represented the optimal conditions for the melt-spinning process. The precursor fiber generated at the optimal condition showed an average diameter of 15.27 ± 3.50 μm.

Furthermore, the thermostabilization and carbonization processes were optimized to yield carbon fiber with an average diameter of 12.66 ± 3.06 μm. The resulting asphaltene-derived carbonized fiber displayed mechanical properties comparable to recently produced carbon fibers derived from pitch or hard/soft woods, with an UTS of 524.07 ± 218.53 MPa, an elastic modulus of 34.68 ± 15.61 GPa, and a strain at the UTS of 2.48 ± 0.97%. This study demonstrates the practical potential of melt-spun asphaltene-based carbon fibers, offering a more streamlined production process and most importantly utilization of low-cost precursor material.

■ ASSOCIATED CONTENT

Supporting Information

The Supporting Information is available free of charge at https://pubs.acs.org/doi/10.1021/acsomega.4c06464.

Fiber morphology after two-step thermostabilization; CHNS/O analysis of cleaned SA and LA; and SEM image and EDX mapping of a cross-section of the precursor fiber in the epoxy matrix (PDF)

■ AUTHOR INFORMATION

Corresponding Author

Cagri Ayranci − *Department of Mechanical Engineering, University of Alberta, Edmonton, Alberta T6G 2R3, Canada;* orcid.org/0000-0002-9638-4445; Email: cayranci@ualberta.ca

Authors

Shahrad Khodaei Booran − *Department of Mechanical Engineering, University of Alberta, Edmonton, Alberta T6G 2R3, Canada;* orcid.org/0000-0003-2840-4018

Jiawei Chen − *Department of Mechanical Engineering, University of Alberta, Edmonton, Alberta T6G 2R3, Canada;* orcid.org/0000-0003-1381-3046

Md Minhajul Islam − *Department of Mechanical Engineering, University of Alberta, Edmonton, Alberta T6G 2R3, Canada; Department of Chemistry, University of Alberta, Edmonton, Alberta T6G 2R3, Canada;* orcid.org/0009-0000-9633-2947

Idaresit Ekaette − *Department of Mechanical Engineering, University of Alberta, Edmonton, Alberta T6G 2R3, Canada*

TriDung Ngo − *InnoTech Alberta, Edmonton, Alberta T6N 1E4, Canada*

Mark McDermott − *Department of Chemistry, University of Alberta, Edmonton, Alberta T6G 2R3, Canada*

Tian Tang − *Department of Mechanical Engineering, University of Alberta, Edmonton, Alberta T6G 2R3, Canada*

Complete contact information is available at: https://pubs.acs.org/10.1021/acsomega.4c06464

Notes

The authors declare no competing financial interest.

■ ACKNOWLEDGMENTS

The authors acknowledge that this work was part of the "Carbon Fiber Grand Challenge" project (212200031), funded by the Clean Resource Innovation Network (CRIN) and Alberta Innovates.

■ REFERENCES

(1) Zhang, J.; Lin, G.; Vaidya, U.; Wang, H. Past, Present and Future Prospective of Global Carbon Fibre Composite Developments and Applications. *Compos. B Eng.* **2023**, *250*, 110463.

(2) Yusof, N.; Ismail, A. F. Post Spinning and Pyrolysis Processes of Polyacrylonitrile (PAN)-Based Carbon Fiber and Activated Carbon Fiber: A Review. *J. Anal. Appl. Pyrolysis* **2012**, *93*, 1−13.

(3) Sunil, S.; Abhilas, J. K.; Kumar, A.; Shukla, H. K. Oxidative Stabilization Studies on Pretreated Polyacrylonitrile Precursor Fiber Suitable for Carbon Fiber. *Production* **2019**, *2166*, 020018.

(4) Mainka, H.; Täger, O.; Körner, E.; Hilfert, L.; Busse, S.; Edelmann, F. T.; Herrmann, A. S. Lignin − an Alternative Precursor for Sustainable and Cost-Effective Automotive Carbon Fiber. *J. Mater. Res. Technol.* **2015**, *4* (3), 283−296.

(5) Wu, Q.; Pan, D. A New Cellulose Based Carbon Fiber from a Lyocell Precursor. *Text. Res. J.* **2002**, *72* (5), 405−410.

(6) Alcañiz-Monge, J.; Cazorla-Amorós, D.; Linares-Solano, A.; Oya, A.; Sakamoto, A.; Hosm, K. Preparation of General Purpose Carbon Fibers from Coal Tar Pitches with Low Softening Point. *Carbon* **1997**, *35* (8), 1079−1087.

(7) Zuo, P.; Leistenschneider, D.; Kim, Y.; Ivey, D. G.; Chen, W. The Effect of Thermal Pretreatment Temperature on the Diameters and Mechanical Properties of Asphaltene-Derived Carbon Fibers. *J. Mater. Sci.* **2021**, *56* (27), 14964−14977.

(8) Leistenschneider, D.; Zuo, P.; Kim, Y.; Abedi, Z.; Ivey, D. G.; de Klerk, A.; Zhang, X.; Chen, W. A Mechanism Study of Acid-Assisted Oxidative Stabilization of Asphaltene-Derived Carbon Fibers. *Carbon Trends* **2021**, *5*, 100090.

(9) Saad, S.; Zeraati, A. S.; Roy, S.; Saadi, M. A. S. R.; Radović, J. R.; Rajeev, A.; Miller, K. A.; Bhattacharyya, S.; Larter, S. R.; Natale, G.; Sundararaj, U.; Ajayan, P. M.; Rahman, M. M.; Kibria, M. G. Transformation of Petroleum Asphaltenes to Carbon Fibers. *Carbon* **2022**, *190*, 92−103.
(10) Chacón-Patiño, M. L.; Neumann, A.; Rüger, C. P.; Bomben, P. G.; Friederici, L.; Zimmermann, R.; Frank, E.; Kreis, P.; Buchmeiser, M. R.; Gray, M. R. Chemistry and Properties of Carbon Fiber Feedstocks from Bitumen Asphaltenes. *Energy Fuels* **2023**, *37* (7), 5341−5360.
(11) Zuo, P.; Leistenschneider, D.; Kim, Y.; Abedi, Z.; Ivey, D. G.; Zhang, X.; Chen, W. Asphaltene Thermal Treatment and Optimization of Oxidation Conditions of Low-Cost Asphaltene-Derived Carbon Fibers. *J. Ind. Eng. Chem.* **2021**, *104*, 427−436.
(12) Gharbi, K.; Benyounes, K.; Khodja, M. Removal and Prevention of Asphaltene Deposition during Oil Production: A Literature Review. *J. Pet. Sci. Eng.* **2017**, *158*, 351−360.
(13) Keshavarz, B.; Dehaghani, A. H. S.; Dehghani, S. A. M. Investigation the Impact of Additives on the Displacement of the Onset Point of Asphaltene Precipitation Using Interfacial Tension Measurement. *Energy Sources, Part A Recovery, Util. Environ. Eff.* **2019**, *41* (11), 1360−1371.
(14) Silva, H. S.; Alfarra, A.; Vallverdu, G.; Bégué, D.; Bouyssiere, B.; Baraille, I. Asphaltene Aggregation Studied by Molecular Dynamics Simulations: Role of the Molecular Architecture and Solvents on the Supramolecular or Colloidal Behavior. *Pet. Sci.* **2019**, *16* (3), 669−684.
(15) Speight, J. G. *The Chemistry and Technology of Petroleum*; CRC Press, 2006.
(16) Marshall, A. G.; Rodgers, R. P. Petroleomics: Chemistry of the Underworld. *Proc. Natl. Acad. Sci. U.S.A.* **2008**, *105* (47), 18090−18095.
(17) Wiehe, I. A.; Liang, K. S. Asphaltenes, Resins, and Other Petroleum Macromolecules. *Fluid Phase Equilib.* **1996**, *117* (1−2), 201−210.
(18) Vilaplana-Ortego, E.; Alcañiz-Monge, J.; Cazorla-Amorós, D.; Linares-Solano, A. Stabilisation of Low Softening Point Petroleum Pitch Fibres by HNO3. *Carbon* **2003**, *41* (5), 1001−1007.
(19) Kim, Y.; Leistenschneider, D.; de Klerk, A.; Chen, W. Rigorous Deasphalting, Autoxidation, and Bromination Pretreatment Methods for Oilsands Bitumen Derived Asphaltenes to Improve Carbon Fiber Production. *Energy Fuels* **2021**, *35* (21), 17463−17478.
(20) Islam, M. M.; Chen, J.; Ekaette, I.; Shahriar, K. A.; Booran, S. K.; Ngo, T.; Tang, T.; McDermott, M. T.; Ayranci, C. Asphaltene-Based Discontinuous Carbon Fiber. *Energy Fuels* **2024**, *38* (15), 14526−14533.
(21) Browne, E.; Worku, Z. A.; Healy, A. M. Physicochemical Properties of Poly-Vinyl Polymers and Their Influence on Ketoprofen Amorphous Solid Dispersion Performance: A Polymer Selection Case Study. *Pharmaceutics* **2020**, *12* (5), 433.
(22) Zhang, Y.; Takanohashi, T.; Sato, S.; Saito, I.; Tanaka, R. Observation of Glass Transition in Asphaltenes. *Energy Fuels* **2004**, *18* (1), 283−284.
(23) Zojaji, I.; Esfandiarian, A.; Taheri-Shakib, J. Toward Molecular Characterization of Asphaltene from Different Origins under Different Conditions by Means of FT-IR Spectroscopy. *Adv. Colloid Interface Sci.* **2021**, *289*, 102314.
(24) Wang, Y.; Alsmeyer, D. C.; McCreery, R. L. Raman Spectroscopy of Carbon Materials: Structural Basis of Observed Spectra. *Chem. Mater.* **1990**, *2* (5), 557−563.
(25) Xu, K. Toward Value-Added Applications of Asphaltenes, **2019**. .
(26) Maslova, O. A.; Ammar, M. R.; Guimbretière, G.; Rouzaud, J.-N.; Simon, P. Determination of Crystallite Size in Polished Graphitized Carbon by Raman Spectroscopy. *Phys. Rev. B:Condens. Matter Mater. Phys.* **2012**, *86* (13), 134205.
(27) Vázquez-Santos, M. B.; Geissler, E.; László, K.; Rouzaud, J.-N.; Martínez-Alonso, A.; Tascón, J. M. D. Comparative XRD, Raman, and TEM Study on Graphitization of PBO-Derived Carbon Fibers. *J. Phys. Chem. C* **2012**, *116* (1), 257−268.
(28) Nunna, S.; Maghe, M.; Rana, R.; Varley, R.; Knorr, D.; Sands, J.; Creighton, C.; Henderson, L.; Naebe, M. Time Dependent Structure and Property Evolution in Fibres during Continuous Carbon Fibre Manufacturing. *Materials* **2019**, *12* (7), 1069.
(29) Luhrs, C.; Moberg, M.; Maxson, A.; Brewer, L.; Menon, S. IF-WS2/Nanostructured Carbon Hybrids Generation and Their Characterization. *Inorganic* **2014**, *2* (2), 211−232.
(30) Wang, S.; Chen, Z.-H.; Ma, W.-J.; Ma, Q.-S. Influence of Heat Treatment on Physical−Chemical Properties of PAN-Based Carbon Fiber. *Ceram. Int.* **2006**, *32* (3), 291−295.
(31) Joshi, K.; Arefev, M. I.; Zhigilei, L. V. Generation and Characterization of Carbon Fiber Microstructures by Atomistic Simulations. *Carbon* **2019**, *152*, 396−408.
(32) Xiang, C.; Behabtu, N.; Liu, Y.; Chae, H. G.; Young, C. C.; Genorio, B.; Tsentalovich, D. E.; Zhang, C.; Kosynkin, D. V.; Lomeda, J. R.; Hwang, C.-C.; Kumar, S.; Pasquali, M.; Tour, J. M. Graphene Nanoribbons as an Advanced Precursor for Making Carbon Fiber. *ACS Nano* **2013**, *7* (2), 1628−1637.
(33) Bourrat, M. A. X. New Carbons, Structure and Applications. *Key Eng. Mater.* **2004**, *264*−*268*, 2261−2266.
(34) Prauchner, M. J.; Pasa, V. M. D.; Otani, S.; Otani, C. Biopitch-Based General Purpose Carbon Fibers: Processing and Properties. *Carbon* **2005**, *43* (3), 591−597.
(35) Baker, D. A.; Gallego, N. C.; Baker, F. S. On the Characterization and Spinning of an Organic-purified Lignin toward the Manufacture of Low-cost Carbon Fiber. *J. Appl. Polym. Sci.* **2012**, *124* (1), 227−234.
(36) Li, P.-P.; Xiong, J.-M.; Ge, M.-L.; Sun, J.-C.; Zhang, W.; Song, Y.-Y. Preparation of Pitch-Based General Purpose Carbon Fibers from Catalytic Slurry Oil. *Fuel Process. Technol.* **2015**, *140*, 231−235.
(37) Steudle, L. M.; Frank, E.; Ota, A.; Hageroth, U.; Henzler, S.; Schuler, W.; Neupert, R.; Buchmeiser, M. R. Carbon Fibers Prepared from Melt Spun Peracylated Softwood Lignin: An Integrated Approach. *Macromol. Mater. Eng.* **2017**, *302* (4), 1600441.

https://doi.org/10.1021/acsomega.4c06464
ACS Omega 2024, 9, 50318−50325